Letters

Nonsingular Sliding Mode Control of PMSM-Drive Servo Systems: A Novel Fast Fixed-Time Scheme

Simeng Song, *Graduate Student Member, IEEE*, Zhilin Liu, and Shouzheng Yuan

***Abstract*—Traditional finite-time/fixed-time control methods have been extensively studied due to their ability to quantitatively determine the settling time of a system. However, these approaches have several drawbacks, such as slow convergence rates, state-dependent settling times, and low control precision. To address these limitations, this article presents an innovative fast fixed-time control theory based on a variable exponential strategy. This approach significantly improves the practical convergence speed and control accuracy, while eliminating the drawback of state-dependent settling time inherent in conventional finite-time control frameworks. Leveraging the proposed theory, a high-precision fast fixed-time sliding mode control scheme is developed for permanent magnet synchronous motors. This methodology significantly improves control accuracy and reduces practical convergence time through the variable exponential strategy. Lyapunov stability analysis proves that the closed-loop tracking error can converge rapidly to an ultra-small neighborhood near the origin within a fixed time. Experimental results further validate the superiority of the proposed scheme, demonstrating exceptional performance in key metrics, including convergence speed and control accuracy. The latter achieves an enhancement of up to 55.1%. Compared with existing fixed-time control approaches, this approach has greater research significance and application potential, providing the technical basis for wider power electronics control applications.**

***Index Terms*—Fixed time convergence, permanent magnet synchronous motor (PMSM), position tracking control, sliding mode control.**

I. Introduction

Owing to advantages, such as high power density, energy efficiency, and compact structure, permanent magnet synchronous motors (PMSMs) are widely used in electric vehicles and robotics, driving significant research interest [1]. Settling time is a critical performance metric for evaluating system performance. In common servo system scenarios, such as obstacle avoidance, strict requirements are placed on settling time. Position control is an important area of research in PMSM servo control systems and has produced many advanced results. However, it remains challenging to achieve both rapid convergence and high precision within strict time constraints.

In [2], a common super-twisting slide mode control was proposed for speed regulation in PMSMs. The settling time of the system was also studied in depth to prove that it is finite-time stable. Repeated adjustment of parameters is required under varying initial conditions, thereby increasing the complexity of engineering implementation. Consequently, achieving a desired settling time requires parameter adjustments for different initial conditions, increasing implementation complexity in practice. To address the inherent limitations of finite-time theory, fixed-time control was proposed, where the settling time is bounded by a constant independent of the initial state and determined solely by the controller parameters. Given the advantages of fixed-time theory, several high-quality research studies have been reported. For example, in [3], a fixed-time sliding mode controller was designed to improve system performance and guarantee error convergence within a fixed time. Larger power exponents accelerate convergence for significant error, and vice versa. However, the fixed-time scheme in [3] cannot adjust the power exponents to adapt to the error, thereby limiting convergence speed.

Recent advances have demonstrated significant progress in combined finite-time/fixed-time sliding mode control for more complex systems, offering enhanced robustness. For servo motor systems, a finite-time continuous terminal sliding mode scheme has been developed to ensure that system states reach the sliding surface within a finite time while maintaining robustness [4]. In [5], the singular perturbation approach was employed to decouple fast–slow subsystems in flexible-joint robots, where an extended state observer integrated with fixed-time integral sliding mode was used to achieve fixed-time convergence of tracking errors under external disturbances, parameteric uncertainties, nonlinearities, and unmodeled dynamics. In [6], the combination of a fixed-time sliding mode observer and a novel fixed-time sliding mode control scheme enables tracking errors of aerial flexible-joint robots to approach zero within a fixed time.

Received 2 October 2025; revised 12 November 2025; accepted 2 December 2025. Date of publication 10 December 2025; date of current version 19 January 2026. This work was supported in part by the Longitudinal Motion Mechanism Analysis and Adaptive Stability Control Method of High-speed Multihull Vessel under Grant 52471320, in part by the Special Project for Industrial Foundation Reconstruction and High Quality Development of Manufacturing Industry by the Ministry of Industry and Information Technology under Grant TC220A04X-1, in part by the HEU Presidential Innovation Fund for Ph.D. Students, and in part by the HEU CISSE Decanal Innovation Fund for Ph.D. Students. *(Corresponding author: Zhilin Liu.)*

Simeng Song and Zhilin Liu are with the College of Intelligent Systems Science and Engineering, Harbin Engineering University, Harbin 150001, China (e-mail: Sssiw6_Echo@ieee.org; liuzhilin@hrbeu.edu.cn).

Shouzheng Yuan is with the China Ship Scientific Research Center, Wuxi 214082, China, and also with the Taihu Laboratory of Deepsea Technological Science, Wuxi 214082, China (e-mail: ysz199606@hrbeu.edu.cn).

Color versions of one or more figures in this article are available at https://doi.org/10.1109/TPEL.2025.3642331.

Digital Object Identifier 10.1109/TPEL.2025.3642331

Although the aforementioned approaches have significantly advanced the development and application of fixed/finite-time control, improvements are still needed in two key areas. First, the power exponents in existing fixed-time theories are predominantly constant, lacking the ability to select suitable exponents dynamically across different error regions to achieve faster convergence speeds and higher control accuracy. Second, the estimated upper bounds of settling time derived from these theories yield overly conservative values, resulting in significant discrepancies between theoretical predictions and practical implementations and thereby compromising the credibility of parameter selection and performance outcomes. Driven by these considerations, the core motivation of this article is to establish a novel fast fixed-time theoretical framework through an innovative variable exponential strategy. This approach simultaneously achieves: 1) accelerated global convergence speed across the entire error region; 2) significant reduction of the estimation gap between theoretical and actual settling times; and 3) experimental validation on PMSM-drive servo systems—highly sensitive platforms demanding both rapid convergence and high control precision.

The main contributions of this article are summarized below, based on the above analysis and motivation.

1) First, we propose a novel fast fixed-time theory with a variable exponential strategy (FFTVES), supported by a rigorous fixed-time convergence proof. The variable exponent mechanism autonomously selects appropriate power exponents across different error regions, thereby accelerating convergence speed. Compared to existing fixed-time theories [7], [8], [9], under identical parameter configurations, the FFTVES achieves faster error convergence, with gains of up to 65.8.
2) Introducing the incomplete beta function ratio for upper bound estimation of settling time significantly enhances estimation accuracy, achieving closer alignment between theoretical predictions and experimentally measured settling times, which reduces parameter tuning trial-and-error costs. Compared to conventional fixed-time theory [8], the accuracy of settling time estimation can be improved by 77.4%.
3) Building upon the FFTVES, we have developed a novel fast fixed-time sliding mode controller for PMSM position servo systems. This controller guarantees position tracking error convergence to a parameter-determined small neighborhood within a fixed time. Experimental comparisons against state-of-the-art fixed-time theories [7], [8], [9] demonstrate superior performance, with faster convergence and improved control accuracy of up to 55.1%.

The sign function is denoted by $\mathrm{sign}(\cdot)$ throughout this article, and we define $\mathrm{sig}^{\varsigma}(\cdot) = |\cdot|^{\varsigma}\mathrm{sign}(\cdot)$, and $\varsigma > 0$.

II. Model Description and Preliminaries

A. Model Description and Assumptions

To simplify controller design, we specify the desired stator current for the d-axis as $i_d^* = 0$. We can describe the mathematical model of the simplified PMSM as follows, assuming effective d-axis current control maintains $i_d = i_d^* = 0$ [2]:

$$\begin{cases} \dot{\theta}_a = \omega_a \\ \dot{\omega}_a = -\frac{\zeta_b}{J}\omega_a + \frac{\zeta_m}{J} i_q - \frac{F_l}{J} \end{cases} \tag{1}$$

where θ_a and ω_a denote the mechanical position and angular velocity, respectively. $\zeta_m = \frac{3p_a\varphi_\varepsilon}{2J}$, where p_a denotes the pole-pair and φ_ε is the rotor flux linkage. J represents the moment of inertia. ζ_b is the viscous frictional coefficient. i_q is represented as the stator current of the q-axis. F_l denotes the load torque.

We use θ_s to represent the desired position angle, and then we can define the tracking error e_1 and its derivative e_2 as follows:

$$\begin{cases} e_1 = \theta_a - \theta_s \\ e_2 = \omega_a - \dot{\theta}_s. \end{cases} \tag{2}$$

To facilitate controller design and analysis, we define $F_d = -\frac{\zeta_b}{J}\omega_a - \frac{F_l}{J}$ as the system's lumped disturbance.

Assumption 1 (see [10]): The lumped disturbance F_d is bounded. There exists a known finite positive constant D_l that satisfies $|F_d| \le D_l$.

Assumption 2 (see [11]): Both θ_s and $\dot{\theta}_s$ are continuously differentiable and bounded. In addition, $\ddot{\theta}_s$ is also bounded.

B. Lemmas

Consider a generalized nonlinear system $\dot{x} = \varphi(x(t))$, where x is the state and $\varphi(\cdot)$ is a nonlinear function. We define $V(x)$ as a Lyapunov function of the system. The following lemma then applies.

Lemma 1: If $V(x)$ satisfying $\dot{V} \le -(a_1V^{\lambda_1} + a_2V^{\lambda_2} + a_3V^{\lambda_3})/\chi(x)$, where $\lambda_1 = 1 + \mu_1(1 + \mathrm{sign}(V-1))/(2\mu_2)$, $\lambda_2 = 1 + \mu_3\mathrm{sign}(V-1)/\mu_4$, $\lambda_3 \in (0,1)$, $\chi(x) = b_1(1 - \mathrm{sech}(b_2|x|^{b_3})) + \mathrm{sech}(b_2|x|^{b_3})$, $b_1 \in (0,1)$, and $\mu_1 > \mu_2$, $\mu_3 < \mu_4$, a_1, a_2, a_3, and b_2 are positive constants, b_3 is a positive even integer, and μ_1, μ_2, μ_3, and μ_4 are positive odd integers, then the system is fixed-time stable.

Proof: The key to this proof is to determine the settling time of the system and demonstrate that it is solely dependent on the parameters and not the system state. To this end, similar to [8], we can obtain settling time $T(x_0)$ satisfying

$$\begin{aligned} T(x_0) &= \int_0^{V(x_0)} \frac{\chi(x)}{a_1V^{\lambda_1} + a_2V^{\lambda_2} + a_3V^{\lambda_3}} dV \\ &\le \int_0^{+\infty} \frac{1}{a_1V^{\lambda_1} + a_2V^{\lambda_2} + a_3V^{\lambda_3}} dV \end{aligned} \tag{3}$$

where x_0 is the initial state of the system. Splitting the integral in (3) yields

$$\begin{aligned} T(x_0) \le & \int_0^1 \frac{1}{a_2V^{1-\frac{\mu_3}{\mu_4}} + a_3V^{1+\lambda_3}} dV \\ & + \int_1^{+\infty} \frac{1}{a_1V^{1+\frac{\mu_1}{\mu_2}} + a_2V^{1+\frac{\mu_3}{\mu_4}-\lambda_3}} dV. \end{aligned} \tag{4}$$

By $m = a_3/(a_2V^{-(\lambda_3+\mu_3/\mu_4)} + a_3)$, we have

$$T_\alpha = \int_0^1 \frac{1}{a_2V^{1-\frac{\mu_3}{\mu_4}} + a_3V^{1+\lambda_3}} dV = \frac{1}{a_3\left(\lambda_3 + \frac{\mu_3}{\mu_4}\right)}$$

$$\left(\frac{a_3}{a_2}\right)^{\frac{\mu_4\lambda_3}{\mu_4\lambda_3+\mu_3}} \int_0^{\frac{a_3}{a_2+a_3}} m^{-\frac{\mu_4\lambda_3}{\mu_4\lambda_3+\mu_3}}(1-m)^{-\frac{\mu_3}{\mu_4\lambda_3+\mu_3}}$$
$$\leq \frac{\mu_4\pi\csc\left(\frac{\pi\mu_4\lambda_3}{\mu_4\lambda_3+\mu_3}\right)}{a_3\left(\lambda_3\mu_4+\mu_3\right)}\left(\frac{a_3}{a_2}\right)^{\frac{\mu_4\lambda_3}{\mu_4\lambda_3+\mu_3}}$$
$$I\left(\frac{a_3}{a_2+a_3},\frac{\mu_3}{\mu_4\lambda_3+\mu_3},\frac{\mu_4\lambda_3}{\mu_4\lambda_3+\mu_3}\right) \tag{5}$$

where $I(\cdot)$ is the incomplete beta function ratio (see [8]). Let $n = (a_2V^{1+\mu_3/\mu_4-\lambda_3})/(a_1V^{1+\mu_1/\mu_2}+a_2V^{1+\mu_3/\mu_4-\lambda_3})$, similar to (5), we can obtain

$$T_\beta = \int_1^{+\infty}\frac{1}{a_1V^{1+\frac{\mu_1}{\mu_2}}+a_2V^{1+\frac{\mu_3}{\mu_4}-\lambda_3}}dV$$
$$\leq \frac{\pi\mu_2\mu_4\csc(\pi p)}{a_2\left(\mu_1\mu_4+\lambda_3\mu_2\mu_4-\mu_2\mu_3\right)}\left(\frac{a_2}{a_1}\right)^{1-p}$$
$$I\left(\frac{a_2}{a_2+a_1},p,1-p\right) \tag{6}$$

where $p = \mu_1\mu_4/(\mu_1\mu_4+\lambda_3\mu_2\mu_4-\mu_2\mu_3)$. In view of (5) and (6), we find that both T_α and T_β are related only to the parameters, rather than the state. Let $T_\gamma = T_\alpha + T_\beta$. Obviously, T_γ is also related only to the parameters and independent of the system state. Considering $T(x_0) \leq T_\gamma$, the conclusion is that the system converges to the origin within the settling time T_γ. This completes the proof. ■

Remark 1: The FFTVES is compared with existing fixed-time schemes [7], [8], [9]. In [9], $V(x)$ must satisfy condition $\dot{V} \leq -(a_1V^{\mu_1/\mu_1}+a_2V^{1-\mu_3/\mu_4})$. Unlike [9], our FFTVES incorporates an adaptive exponent strategy that adjusts the corresponding index based on different $V(x)$. This accelerates the system's convergence speed. Specifically, when $V > 1$, the aim is to maximize the exponents to accelerate convergence. Conversely, when $V < 1$, the aim is to minimize the exponents for the same reason. Adding the term $a_3V^{\lambda_3}$ further enhances convergence speed and reduces the actual settling time. In [7], $V(x)$ needs to satisfy $\dot{V} \leq -(a_1V^{\lambda_4}+a_2V^{1-\mu_3/\mu_4})/\vartheta(x)$, where $\vartheta(x) = (b_1+(1-b_1))e^{-b_2|x|^{b_3}}$ and $\lambda_4 = 0.5+\mu_1/\mu_2+(\mu_1/\mu_2-0.5)\text{sign}(V-1)$. Compared to [7], our FFTVES achieves faster convergence because it also incorporates a variable exponential strategy for item $a_2V^{\lambda_2}$ and includes item $a_2V^{\lambda_2}$. In [8], $V(x)$ needs to satisfy $\dot{V} \leq -(a_1V^{1+\mu_1/\mu_2}+a_2V^{1+\mu_3/\mu_4}+a_3V^{\lambda_3})$. Compared to [8], our scheme reduces the actual settling time by employing a variable exponential strategy and incorporating term $\chi(x)$. In addition, the system's antidisturbance capability has been improved to a certain extent due to the addition of item $a_3V^{\lambda_3}$, compared with [7] and [9].

To further verify that the convergence rate of our Lemma 1 is faster and the settling time is shorter than that of the schemes in [7], [8], and [9], we conducted a fair comparison by selecting the same parameters. These parameters are set to $a_1 = a_2 = a_3 = 2$, $\mu_1 = 9$, $\mu_2 = 5$, $\mu_3 = 7$, $\mu_4 = 9$, $\lambda_3 = 0.9$, $b_1 = 0.8$, $b_2 = 10$, and $b_3 = 2$. The results of the comparison are shown in Fig. 1. Clearly, our scheme has the fastest convergence speed

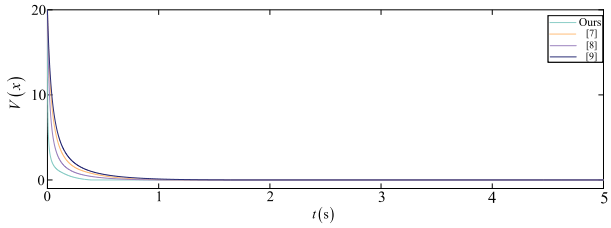

Fig. 1. Comparison of convergence performance under four fixed-time schemes.

and shortest settling time of all the schemes. Specifically, the actual settling times under ours, [8], [7], and [9] are 0.411, 1.201, 1.558, and 1.571 s, respectively. Even when compared to the relatively superior scheme [8], it is evident that our scheme can reduce the settling time by a further 65.8%. Furthermore, we would like to emphasize that the theoretical settling time calculated via our estimated upper bound (5) and (6) is 0.706 s. Whereas the theoretical settling time calculated via [9] is 2.876 s. Therefore, we conclude that our proposed novel fixed-time theory can reduce the estimation error of the upper bound of the settling time by 77.4%.

Remark 2: Through the analysis outlined in Remark 1 and by comparing simulations, we conclude that the novel FFTVES has the following three distinct advantages over other fixed-time theories [7], [8], [9]. First, the incorporation of a variable exponential strategy enables the FFTVES to converge faster under identical conditions than other fixed-time theories, thereby enhancing the system's dynamic performance. Second, compared to the scheme in [7] and [9], the FFTVES incorporates an additional robustness term, $a_3V^{\lambda_3}$, that accelerates convergence and improves the system's antidisturbance capability. Third, the introduction of the incomplete beta function ratio means that the upper bound estimate for settling time under the FFTVES more closely approximates the actual value than other theories do, which facilitates more effective user adjustment and system performance planning.

III. Design of Novel Fixed-Time Sliding Mode Control

A. Controller Design

The novel fixed-time sliding mode manifold with adaptive exponents is designed as follows:

$$s = e_2 + \frac{1}{\chi(e_1)}\left(k_1\text{sig}^{\beta_1}(e_1)+k_2R_1(e_1)+k_3R_2(e_1)\right) \tag{7}$$

where $\beta_1 = 1+(1+\text{sign}(|e_1|-1))\mu_1/\mu_2$, and k_1, k_2, and k_3 are positive constants. $R_1(e_1)$ is

$$R_1(e_1) = \begin{cases}\text{sig}^{\beta_2}(e_1), \text{if } \tilde{s}=0 \text{ or } \tilde{s}\neq 0, |e_1|\geq e_m \\ \nu_1e_1+\nu_2e_1^2\text{sign}(e_1), \text{otherwise}\end{cases} \tag{8}$$

where $\beta_2 = 1+\mu_3\text{sign}(|e_1|-1)/\mu_4$, $\nu_1 = (1+\mu_3/\mu_4)e_m^{-\mu_3/\mu_4}$, and $\nu_2 = -\mu_3/\mu_4e_m^{-\mu_3/\mu_4-1}$. $\tilde{s}$ is defined as

$$\tilde{s}=\frac{1}{\chi\left(e_1\right)}\left(k_1\mathrm{sig}^{\beta_1}\left(e_1\right)+k_2\mathrm{sig}^{\beta_2}\left(e_1\right)+k_3\mathrm{sig}^{\beta_3}\left(e_1\right)\right)+e_2 \tag{9}$$

where β_3 is a positive constant and $\beta_3\in(0,1)$. $R_2(e_1)$ is

$$R_2\left(e_1\right)=\begin{cases}\mathrm{sig}^{\beta_3}\left(e_1\right),\text{if }\ \tilde{s}=0\ \text{ or }\ \tilde{s}\neq 0,\ |e_1|\geq e_m\\ \nu_3 e_1+\nu_4 e_1^2\mathrm{sign}\left(e_1\right),\text{otherwise}\end{cases} \tag{10}$$

where $\nu_3=(2-\beta_3)e_m^{\beta_3-1}$, and $\nu_4=(\beta_3-1)e_m^{\beta_3-2}$. Based on Lemma 1 and the proposed manifold (7), we construct the following new fixed-time sliding mode control law i_q with variable exponents:

$$\begin{aligned}i_q=&-\frac{J}{\zeta_m}\Bigg(D_l\mathrm{sign}(s)-\ddot{\theta}_s+\frac{1}{\chi(s)}\left(k_4\mathrm{sig}^{\beta_1}(s)+\right.\\&k_5\mathrm{sig}^{\beta_2}(s)+k_6\mathrm{sig}^{\beta_3}(s)\Big)-\frac{\dot{\chi}\left(e_1\right)}{\chi^2\left(e_1\right)}\left(k_1\mathrm{sig}^{\beta_1}\left(e_1\right)\right.\\&+k_2R_1\left(e_1\right)+k_3R_2\left(e_1\right)\Big)\\&+\frac{e_2}{\chi\left(e_1\right)}\left(\beta_1k_1|\chi_1|^{\beta_1-1}+k_2\dot{R}_1\left(e_1\right)+k_3\dot{R}_2\left(e_1\right)\right)\Bigg)\end{aligned} \tag{11}$$

where k_4, k_5, and k_6 are controller gain constants.

B. Stability Analysis

Next, we will analyze the stability of the entire closed-loop system.

Theorem 1: For the PMSM (1), under Assumptions 1 and 2, with control law (11), we can conclude that the position tracking error can converge to a small neighborhood of the origin within a fixed time.

Proof: First, a Lyapunov function candidate V_1 is selected as $V_1=s^2/2$. Substituting i_q into $\dot{V}_1$ gives

$$\dot{V}_1\leq-\frac{1}{\chi(s)}\left(k_4|s|^{1+\beta_1}+k_5|s|^{1+\beta_2}+k_6|s|^{1+\beta_3}\right). \tag{12}$$

When $|s|\geq 1$, simplifying (12) to obtain

$$\dot{V}_1\leq-\frac{1}{\chi(s)}\left(\eta_1V_1^{\frac{2\mu_2+\mu_1}{2\mu_2}}+\eta_4V_1^{\frac{2\mu_4+\mu_3}{2\mu_4}}+\eta_3k_6V_1^{\varpi_3}\right). \tag{13}$$

When $|s|<1$, (12) becomes

$$\dot{V}_1\leq-\frac{1}{\chi(s)}\left(2k_4V_1+\eta_2V_1^{\frac{2\mu_4-\mu_3}{2\mu_4}}+\eta_3V_1^{\varpi_3}\right) \tag{14}$$

where $\eta_1=2^{1+0.5\mu_1/\mu_2}k_4$, $\eta_2=2^{1-0.5\mu_3/\mu_4}k_5$, $\eta_3=2^{0.5(1+\beta_3)}k_6$, $\eta_4=2^{1+0.5\mu_3/\mu_4}k_5$, and $\varpi_3=(1+\beta_3)/2$. By combining (13) and (14) with Lemma 1, we can prove that s converges to 0 within a fixed time T_1, where T_1 is described as

$$\begin{aligned}T_1=&\frac{2\mu_4\pi\csc\left(\frac{2\pi\mu_4\varpi_3}{2\mu_4\varpi_3+\mu_3}\right)}{\eta_3\left(2\varpi_3\mu_4+\mu_3\right)}\left(\frac{\eta_3}{\eta_2}\right)^{\frac{2\mu_4\varpi_3}{2\mu_4\varpi_3+\mu_3}}I\left(\frac{\eta_3}{\eta_2+\eta_3},\right.\\&\left.\frac{\mu_3}{2\mu_4\varpi_3+\mu_3},\frac{2\mu_4\varpi_3}{2\mu_4\varpi_3+\mu_3}\right)+I\left(\frac{\eta_4}{\eta_4+\eta_1},p_1,1-p_1\right)\\&\frac{2\pi\mu_2\mu_4\csc\left(\pi p_1\right)}{\eta_4\left(\mu_1\mu_4+2\varpi_3\mu_2\mu_4-\mu_2\mu_3\right)}\left(\frac{\eta_4}{\eta_1}\right)^{1-p_1}.\end{aligned} \tag{15}$$

After T_1, $s=0$. Next, we will discuss three cases.

Case 1: When $\tilde{s}=0$, we have

$$e_2=-\frac{1}{\chi\left(e_1\right)}\left(k_1\mathrm{sig}^{\beta_1}\left(e_1\right)+k_2\mathrm{sig}^{\beta_2}\left(e_1\right)+k_3\mathrm{sig}^{\beta_3}\left(e_1\right)\right). \tag{16}$$

We select a Lyapunov function candidate $V_2=e_1^2/2$. Substituting (16) into $\dot{V}_2$ gives

$$\dot{V}_2\leq\begin{cases}-\frac{1}{\chi(e_1)}\left(2^{\frac{2\mu_2+\mu_1}{2\mu_2}}k_1V_1^{\frac{2\mu_2+\mu_1}{2\mu_2}}+2^{\frac{2\mu_4+\mu_3}{2\mu_4}}k_2V_1^{\frac{2\mu_4+\mu_3}{2\mu_4}}\right.\\\left.+2^{1+\beta_3}k_3V_1^{1+\beta_3}\right),|e_1|\geq 1\\-\frac{1}{\chi(e_1)}\left(2k_1V_1+2^{\frac{2\mu_4-\mu_3}{2\mu_4}}k_2V_1^{\frac{2\mu_4-\mu_3}{2\mu_4}}\right.\\\left.+2^{1+\beta_3}k_3V_1^{1+\beta_3}\right),|e_1|<1\end{cases} \tag{17}$$

where $\eta_5=2^{1+0.5\mu_1/\mu_2}k_1$, $\eta_6=2^{1-0.5\mu_3/\mu_4}k_2$, $\eta_7=2^{0.5(1+\beta_3)}k_3$, and $\eta_8=2^{1+0.5\mu_3/\mu_4}k_2$.

Together with Lemma 1, the conclusion is that the position error e_1 will converge to the origin within $T_2=T_1+T_3$, and T_3 is obtained by replacing η_1, η_2, η_3, and η_4 in T_1 with η_5, η_6, η_7, and η_8, respectively. Case 2: If $\tilde{s}\neq 0$ and $|e_1|\geq e_m$, then it can be seen from the above proof, when the current time t satisfies $t\geq T_2$, $|e_1|<e_m$.

Case 3: If $\tilde{s}\neq 0$ and $|e_1|<e_m$, then it can be seen from the above proof, $|e_1|$ will always remain within $|e_1|<e_m$.

In summary, the tracking error e_1 will converge to a small neighborhood $|e_1|<e_m$ around the origin after $t\geq T_2$. ■

Remark 3: To facilitate parameter adjustment, we provide qualitative guidance on parameter selection here. Specific details are as follows.

For parameters b_1, b_2, and b_3, where $b_1\in(0,1)$, $b_2>0$, and b_3 is a positive even integer, increasing b_2 while decreasing b_1 can accelerate convergence speed, but this requires a larger input and may cause input saturation issues. For b_3, selecting $b_3=2$ is sufficient.

Increasing k_1, k_2, k_3, k_4, k_5, and k_6 will accelerate the system's convergence speed. More significantly, these gains directly determine the system's settling time [see (15)]. However, this may lead to undesirable input saturation and exacerbate chattering. We must make a comprehensive selection based on the task requirements.

The faster the convergence speed achieved, the larger the values of μ_1/μ_2 and μ_3/μ_4, and the smaller the value of β_3. However, the effects of saturation constraints and surges must also be considered.

When adjusting the parameters in practice, we should first select suitable initial values based on the provided parameter set and the required settling time for the task. This selection should be guided by (15) the qualitative analysis above. We should

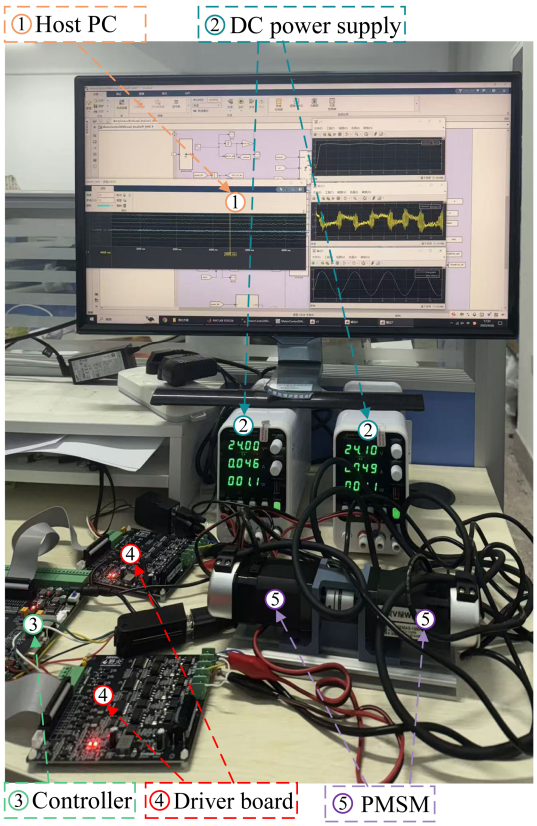

Fig. 2. PMSM towing platform.

then consistently refine control accuracy and convergence speed by sequentially adjusting parameters, bearing in mind that if undesirable effects occur, such as severe chattering, then this indicates a need to reduce the gains.

IV. Experimental Results

All experiments were conducted using a PMSM towing platform (see Fig. 2) consisting of a desktop computer, two PMSMs, an STM32F407-based control board, two drive boards, and two power supplies. The parameters of the platform are $J = 0.28\ \text{kg} \cdot \text{cm}^2$, $p_a = 4$, and $\varphi_\varepsilon = 0.03$ Wb. The other parameters are $k_1 = 2.1$, $k_2 = 2.2$, $k_3 = 1.6$, $k_4 = 8$, $k_1 = 7$, $k_1 = 6$, $\mu_1 = 11$, $\mu_2 = 6$, $\mu_3 = 2$, $\mu_4 = 7$, $e_m = 0.08$, $b_1 = 0.8$, $b_2 = 3$, $b_3 = 2$, and $\theta_s = 3\sin(0.6\pi t) - 1$ rad. For subsequent explanation and comparison, we use SFXTC to represent the scheme in [7], NAFTC to represent the scheme in [8], and CFXTC to represent the scheme in [9]. The scheme we propose is represented by FFXTC. To ensure fairness, all schemes use the same set of parameters.

The experimental results are shown in Figs. 3–6. Fig. 3 shows the position tracking performance under different schemes. Although all four schemes can guarantee the mechanical angle to track the expected angle, it can be seen from the enlarged figure that θ_a under our FFXTC is closest to θ_s. Fig. 4 shows the convergence performance of tracking error under four schemes. Fig. 4 confirms that FFXTC achieves the fastest error convergence and smallest steady-state error. We introduce indicator $\Xi(e_1(t)) = \sum_{\rho=0}^{t} |e_1(\rho)|/t$ to quantify tracking performance under different schemes [12]. The indicators under FFXTC, SFXTC, NAFTC, and CFXTC are 272.3 rad/s, 403.6 rad/s, 372.4 rad/s, and 606.3 rad/s, respectively. FFXTC delivers superior tracking performance compared with other schemes. Furthermore, FFXTC can effectively improve tracking accuracy by 55.1% compared with the worst CFXTC. Fig. 5 shows the response curves of the sliding mode surface under four different schemes. As can be seen, s reaches a steady-state value extremely quickly and is bounded with respect to the origin. Fig. 6 shows the response curves of input i_q under four different schemes.

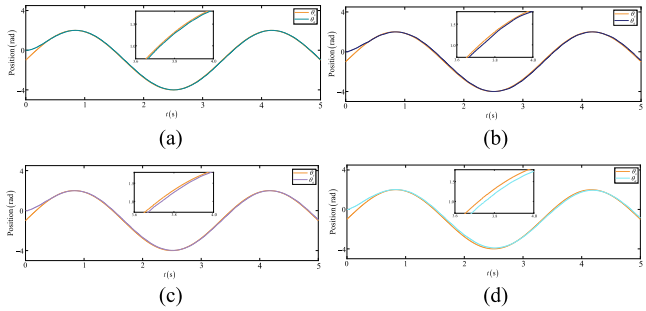

Fig. 3. Mechanical angle tracking performance under different schemes. (a) Position tracking under FFXTC. (b) Position tracking under SFXTC. (c) Position tracking under NAFTC. (d) Position tracking under CFXTC.

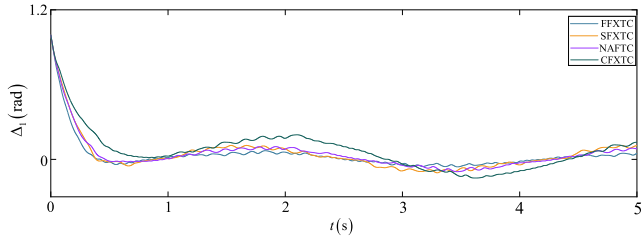

Fig. 4. Tracking error under four schemes.

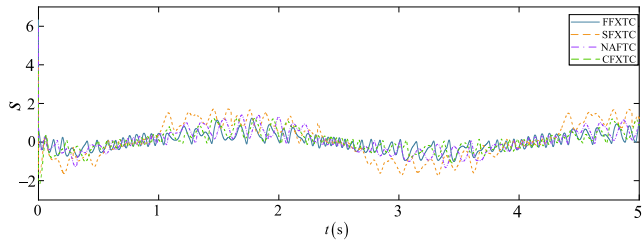

Fig. 5. Sliding mode surface under four schemes.

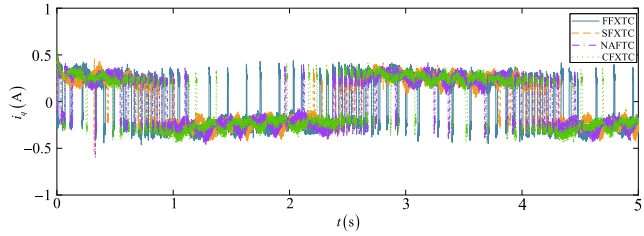

Fig. 6. Input i_q under four schemes.

V. Conclusion

This article proposes a novel fast fixed-time sliding mode control scheme with a variable exponent strategy for PMSM-drive servo systems. This scheme ensures that the position tracking error converges within a fixed time, regardless of the system state, benefiting practical systems requiring strict settling times. The effectiveness of the control scheme has been verified through theoretical analysis and experimental testing in PMSM-drive servo systems. Furthermore, we compare the proposed scheme with the widely used fixed-time schemes. The experimental results confirm that the tracking error converges fastest and achieves the highest accuracy under our scheme. More importantly, our scheme improves control accuracy by 55.1% compared to the worst-performing scheme.

We discuss the limitations and potential challenges of the proposed control scheme. First, we did not consider the limitation of input saturation. This limitation prevents the actual settling time from being arbitrarily small. We have not explored the relationship between these factors in depth. Second, our scheme is significantly dependent on D_l, which could lead to degraded performance when confronted with time-varying upper bound disturbances. Third, our scheme remains sensitive to unmodeled high-frequency dynamics, such as structural resonances and measurement noise, which is a common challenge in sliding-mode control. Future work will focus primarily on addressing the aforementioned limitations and challenges.

References

[1] X. Lin, J. Liu, Z. Liu, Y. Gao, L. Peretti, and L. Wu, "Model-free current predictive control for PMSMs with ultralocal model employing fixed-time observer and extremum-seeking method," *IEEE Trans. Power Electron.*, vol. 40, no. 8, pp. 10682–10693, Aug. 2025.

[2] L. Chen, H. Zhang, H. Wang, K. Shao, G. Wang, and A. Yazdani, "Continuous adaptive fast terminal sliding mode-based speed regulation control of PMSM drive via improved super-twisting observer," *IEEE Trans. Ind. Electron.*, vol. 71, no. 5, pp. 5105–5115, May 2024.

[3] X. Lin et al., "Observer-based fixed-time control for permanent-magnet synchronous motors with parameter uncertainties," *IEEE Trans. Power Electron.*, vol. 38, no. 4, pp. 4335–4344, Apr. 2023.

[4] H. Hou, X. Yu, L. Xu, K. Rsetam, and Z. Cao, "Finite-time continuous terminal sliding mode control of servo motor systems," *IEEE Trans. Ind. Electron.*, vol. 67, no. 7, pp. 5647–5656, Jul. 2020.

[5] R. F. A. Khan, K. Rsetam, Z. Cao, and Z. Man, "ESO based adaptive fixed-time integral sliding mode control for flexible joint robots using singular perturbation method," *Nonlinear Dyn.*, vol. 113, no. 18, pp. 24981–25000, Sep. 2025.

[6] K. Rsetam, Z. Cao, L. Wang, M. Al-Rawi, and Z. Man, "Practically robust fixed-time convergent sliding mode control for underactuated aerial flexible jointrobots manipulators," *Drones*, vol. 6, no. 12, Dec. 2022, Art. no. 428.

[7] M. Gao, L. Ding, and X. Jin, "ELM-based adaptive faster fixed-time control of robotic manipulator systems," *IEEE Trans. Neural Netw. Learn. Syst.*, vol. 34, no. 8, pp. 4646–4658, Aug. 2023.

[8] F. Ren, X. Wang, Y. Li, Z. Chen, C. Wei, and Z. Zeng, "Fixed-time stabilization of multi-weighted complex networks via novel adaptive pinning chatter-free control and its applications," *IEEE Trans. Circuits Syst. I-Regul. Pap.*, vol. 71, no. 6, pp. 2872–2884, Jun. 2024.

[9] S. Song, Z. Liu, S. Yuan, and Z. Wang, "Cascaded extended state observers-based fixed-time line-of-sight path following control for unmanned surface vessels with disturbances and saturation," *IEEE Trans. Veh. Technol.*, vol. 73, no. 6, pp. 7733–7747, Jun. 2024.

[10] S. Shi, L. Dai, H. Min, J. Yang, and S. Li, "Prescribed-time nonsingular terminal sliding mode control and its application in PMSM servo systems," *IEEE Trans. Ind. Electron.*, vol. 72, no. 3, pp. 3072–3081, Mar. 2025.

[11] S. Song, Z. Liu, and L. Yang, "Attitude tracking antidisturbance control for the rigid spacecraft with saturation: A global two-phase prescribed-time approach," *IEEE Trans. Aerosp. Electron. Syst.*, vol. 61, no. 6, pp. 16492–16504, Dec. 2025.

[12] S. Song, Z. Liu, and Z. Wang, "Antidisturbance tracking control of rigid spacecraft attitude systems with saturation and asymmetric constraints," *IEEE Trans. Aerosp. Electron. Syst.*, vol. 61, no. 4, pp. 10336–10348, Aug. 2025.